

## Supporting Information

### Improving cyclability and capacity of Li-O<sub>2</sub> batteries via low rate pre-activation

Zhihong Luo, Guangbin Zhu, Lulu Guo, Fujie Li, Yibing Li, Meng Fu, Yuan-Cheng Cao, Ya-Li Li, Kun Luo

## 1. Experimental

### 1.1 Materials and Chemicals

Multi-walled carbon nanotubes (MWNTs,  $d = 10 \pm 1$  nm,  $L = 3-6$   $\mu\text{m}$ , Sigma-Aldrich), ethanol (>99.7%, AR, Sinopharm), carbon paper (TORAY, TGP-H-060), dimethyl ether (DME, anhydrous, 99.5%, Sigma-Aldrich), lithium carbonate ( $\text{Li}_2\text{CO}_3$ , 99.0%, Sigma-Aldrich) and borosilicate glass fiber filter paper ( $d = 18$  mm, Whatman) were used directly as received. Prior to use, dimethyl sulfoxide (DMSO, anhydrous, 99.9%, Sigma-Aldrich) and propylene carbonate (PC, anhydrous, 99.7%, Sigma-Aldrich) were dehydrated with activated 4Å molecular sieves, and lithium perchlorate ( $\text{LiClO}_4$ , 99.99%, Sigma-Aldrich) was dried at 160 °C in a vacuum oven for 12 h, respectively. Li plates (Shenzhen Poxon Machinery Technology Co. Ltd.) were immersed in 0.1 M  $\text{LiClO}_4/\text{PC}$  solution for at least two days before use.

### 1.2 Li-O<sub>2</sub> battery assembly and testing

3 mg of MWNTs were dispersed in 10 mL ethanol by ultrasonic stirring, and the slurry was sprayed onto carbon paper with a MWNTs loading of 0.1 mg  $\text{cm}^{-2}$ , which was dried in a vacuum oven at 60 °C overnight. The carbon paper with MWNTs was cut to fit the holed CR2032 coin cell, which served as the cathodes in the aprotic Li-O<sub>2</sub> batteries. The coin cell was assembled in an argon-filled glovebox (Mikrouna Co., Ltd.,  $\text{H}_2\text{O} < 0.1$  ppm,  $\text{O}_2 < 0.1$  ppm), where the Li anode, separator and cathode were placed in sequence, followed with the addition of 100  $\mu\text{L}$  DMSO electrolyte containing 1 M  $\text{LiClO}_4$ . The assembled cells were kept in the glovebox overnight, and then were examined by a Battery Testing System (CT-3008W-5V10mA, Neware Technology Co. Ltd., China) in a home-made gas proof container filled with pure oxygen ( $\geq 99.9\%$ , 1.1 atm).

There were two ways of battery testing in the experiments: (1) Direct cycling at 1 A  $\text{g}^{-1}$  with a fixed capacity of 1000 mAh  $\text{g}^{-1}$  till battery failure; (2) Two-step cycling including a 20-cycle pre-activation and a normal cycling. That is, the cell was firstly cycled for 20 times at 0.5 A  $\text{g}^{-1}$  with a fixed capacity of 200 mAh  $\text{g}^{-1}$  based on the loading mass of MWNTs, and then was switched to cycle at 1 A  $\text{g}^{-1}$  with a persistent capacity of 1000 mAh  $\text{g}^{-1}$  till battery failure. For the both cases, the cutoff potentials were set up at 2.0 V and 4.5 V. It was noticed that a few dozens of charge/discharge cycles were required before the battery testing could be commenced, and the cycle numbers in the activation process of the Li-O<sub>2</sub> cells were recorded. The battery testing was performed at 1 A  $\text{g}^{-1}$  with a persistent capacity of 1000 mAh  $\text{g}^{-1}$  in the experiments after the cells

were effectively activated.

The battery testing was also performed at the high current densities of 2 A g<sup>-1</sup>, 3 A g<sup>-1</sup> and 5 A g<sup>-1</sup>, respectively, to investigate the rate performance of the cells. The ultimate capacity was determined by discharging the Li-O<sub>2</sub> cells at 1 A g<sup>-1</sup> to the cutoff potential of 2.0 V. To optimize the parameters of the low rate pre-activation, the cells were tested at the current densities of 0.1, 0.2, 0.5, 1 and 2 A g<sup>-1</sup> with a capacity of 200 mAh g<sup>-1</sup> for 20 cycles, or at the current density of 0.5 A g<sup>-1</sup> with the capacities of 25, 50, 100, 200, 400, 500, 800 and 1000 mAh g<sup>-1</sup> for 20 cycles, or at the current density of 0.5 A g<sup>-1</sup> with the capacities of 200 mAh g<sup>-1</sup> for 5, 10, 20, 30 and 40 cycles.

## 1.2 Characterizations

After battery testing, the coin cells were disassembled in the glove box, and the Li anodes and MWNTs cathodes were removed and rinsed with DME, which were available for further characterization after drying in pure argon atmosphere at room temperature.

The morphology of the MWNTs cathode and Li anode was examined by using a field scanning electron microscopy (SEM, S-4800, Hitachi). X-Ray diffractometer (XRD, X'Pert PRO) equipped with Cu K $\alpha$  radiation was employed to analyse the structure of the solid products on the MWNTs cathodes and Li anodes with a scan rate of 0.6 °/min. The in-depth XPS profiling was carried out by an X-Ray photoelectron spectroscope (XPS, ESCALAB 250Xi, Thermo Fisher Scientific) using Al K $\alpha$  X-ray radiation, and the accelerating voltage of Ar<sup>+</sup> sputtering was settled at 1.0 keV.

Electrochemical impedance spectroscopy (EIS) investigations was fulfilled at different periods of battery testing on an electrochemical workstation (CHI750E, CH instruments), where Ar was aerated in the cells for 30 min to substitute the O<sub>2</sub> for EIS analysis. The measurement was conducted at the open circuit potential of the cell in the frequency range from 0.1 Hz to 1 MHz with the amplitude of 5 mV. The EIS results were interpreted by using the Zview software.

## 2. Supplementary Tables:

**Table S1**  $R_s$ ,  $R_1$  and  $R_2$  values by EIS analysis

Sample	With pre-activation			Without pre-activation		
	$R_s/\Omega$	$R_1/\Omega$	$R_2/\Omega$	$R_s/\Omega$	$R_1/\Omega$	$R_2/\Omega$
20 cycles in the beginning	12.4	95.1	82.7	17.7	110.6	131.1
1 <sup>st</sup> cycle of battery testing	15.5	96.4	158.6	22.7	113.6	315.1
55 <sup>th</sup> cycle of battery testing	112.0	142.8	287.6	136.6	323.3	427.6

**Table S2** Component analysis from XPS in-depth profiling

Sample	Element	Binding Energy /eV	Possible chemistry with Ar <sup>+</sup> etching time					
			0 s	30 s	60 s	90 s	120 s	
Without pre-activation	C	284.8	C-C	C-C	C-C	C-C	C-C	
		288.6	RC*O <sub>2</sub> Li	RC*O <sub>2</sub> Li	RC*O <sub>2</sub> Li	RC*O <sub>2</sub> Li	RC*O <sub>2</sub> Li	
		290.3	--	Li <sub>2</sub> C*O <sub>3</sub>				
	Li	54.8	RCO <sub>2</sub> Li*	RCO <sub>2</sub> Li*/ Li <sub>2</sub> *CO <sub>3</sub>				
		55.2	--	--	Li <sub>2</sub> *O	Li <sub>2</sub> *O	Li <sub>2</sub> *O	
	O	528.6	--	--	Li <sub>2</sub> O*	Li <sub>2</sub> O*	Li <sub>2</sub> O*	
		531.6	RCO <sub>2</sub> *Li	RCO <sub>2</sub> *Li/ Li <sub>2</sub> CO <sub>3</sub> *				
	With pre-activation	C	284.8	C-C	C-C	C-C	C-C	C-C
			288.6	RC*O <sub>2</sub> Li	RC*O <sub>2</sub> Li	RC*O <sub>2</sub> Li	RC*O <sub>2</sub> Li	RC*O <sub>2</sub> Li
290.3			--	Li <sub>2</sub> C*O <sub>3</sub>				
Li		54.8	RCO <sub>2</sub> Li*	RCO <sub>2</sub> Li*/ Li <sub>2</sub> *CO <sub>3</sub>				
		55.2	--	Li <sub>2</sub> *O	Li <sub>2</sub> *O	Li <sub>2</sub> *O	Li <sub>2</sub> *O	
O		528.6	--	Li <sub>2</sub> O*	Li <sub>2</sub> O*	Li <sub>2</sub> O*	Li <sub>2</sub> O*	
		531.6	RCO <sub>2</sub> *Li	RCO <sub>2</sub> *Li/ Li <sub>2</sub> CO <sub>3</sub> *				
Standard Li <sub>2</sub> CO <sub>3</sub>		C	284.8	C-C	--	--	--	--
			290.3	Li <sub>2</sub> C*O <sub>3</sub>	--	--	--	--
	Li	54.8	Li <sub>2</sub> *CO <sub>3</sub>	--	--	--	--	
	O	531.6	Li <sub>2</sub> CO <sub>3</sub> *	--	--	--	--	

### 3. Supplementary Figures:

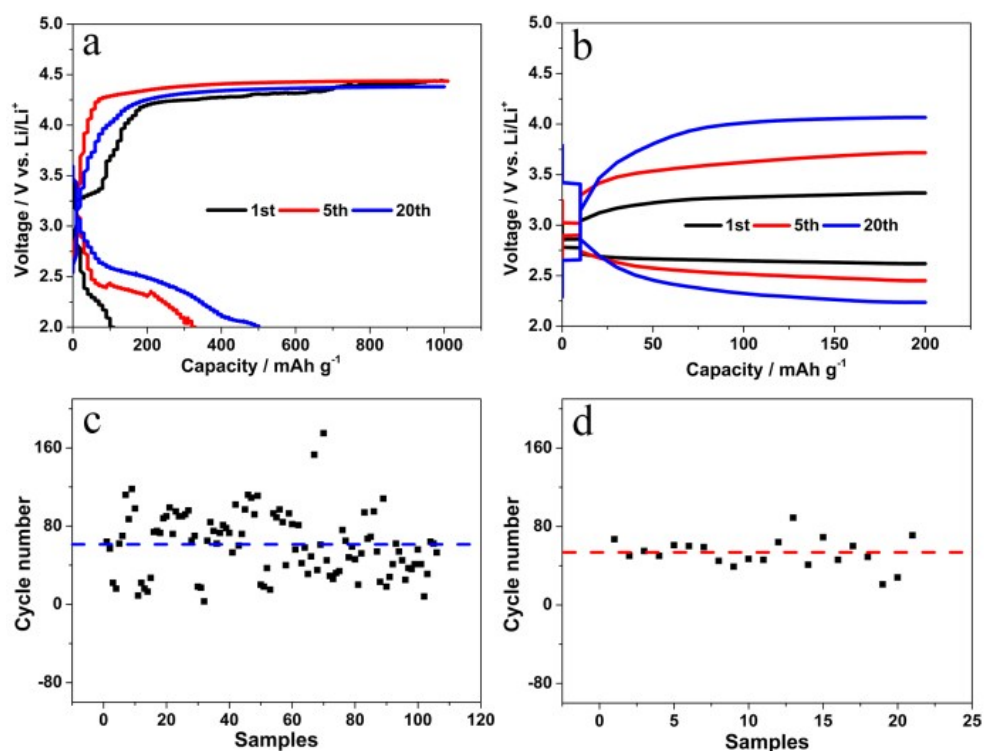


**Fig. S1** 20-cycle profiles at 1 A g<sup>-1</sup> with a capacity of 1000 mAh g<sup>-1</sup> (a) and at 0.5 A g<sup>-1</sup> with a capacity of 200 mAh g<sup>-1</sup> (b, pre-activation). Charge/discharge cycles needed before battery testing could start at the current density of 1 A g<sup>-1</sup> with a fixed capacity of 1000 mAh g<sup>-1</sup> for the cells without pre-activation (c) and the cells with pre-activation (d).

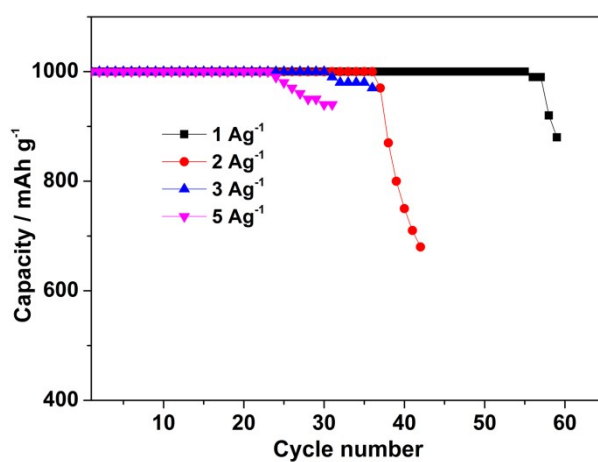


**Fig. S2** Rate performance of the cells without pre-activation at the current densities of 1 A g<sup>-1</sup>, 2 A g<sup>-1</sup>, 3 A g<sup>-1</sup> and 5 A g<sup>-1</sup> with a fixed capacity of 1000 mAh g<sup>-1</sup>.

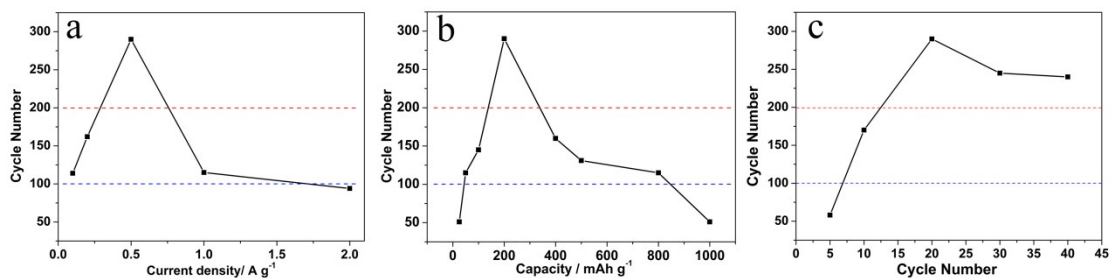


**Fig. S3** The current density (a), capacity (b) and cycle number (c) dependence of the cyclic performance of the Li-O<sub>2</sub> batteries in the low rate pre-activation.

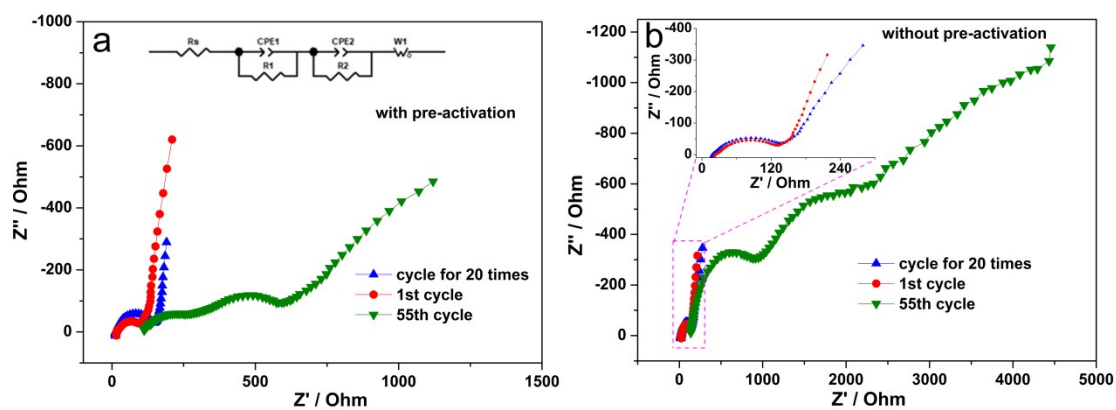


**Fig. S4** Nyquist plots of the cell with (a, inset: equivalent circuit) and without pre-activation (b, inset: local enlargement of the 1<sup>st</sup> and 20<sup>th</sup> cycles).

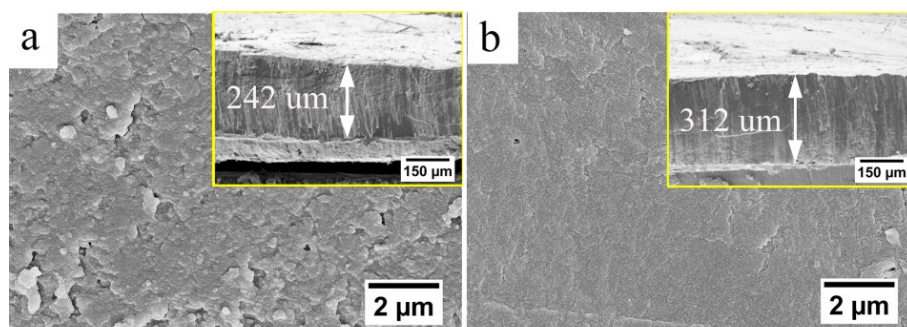


**Fig. S5** SEM images of the anode without pre-activation (a, inset: cross-sectional survey) and with pre-activation (b, inset: cross-sectional survey) at the 1<sup>st</sup> cycle of battery testing.

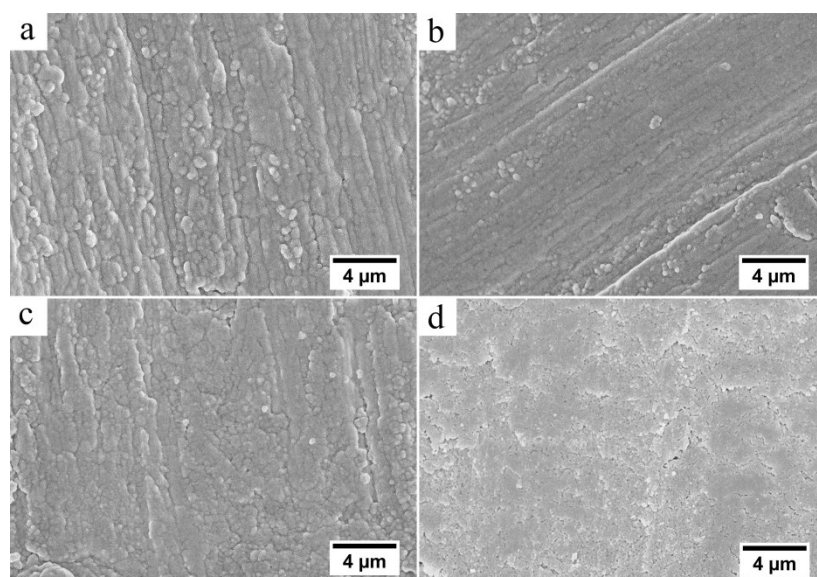


**Fig. S6** SEM images of the Li anodes after 20-cycle pre-activation with fixed capacity of 200 mAh g<sup>-1</sup> at current densities of: a — 0.1 A g<sup>-1</sup>; b — 0.2 A g<sup>-1</sup>; c — 1 A g<sup>-1</sup>; d — 2 A g<sup>-1</sup>.

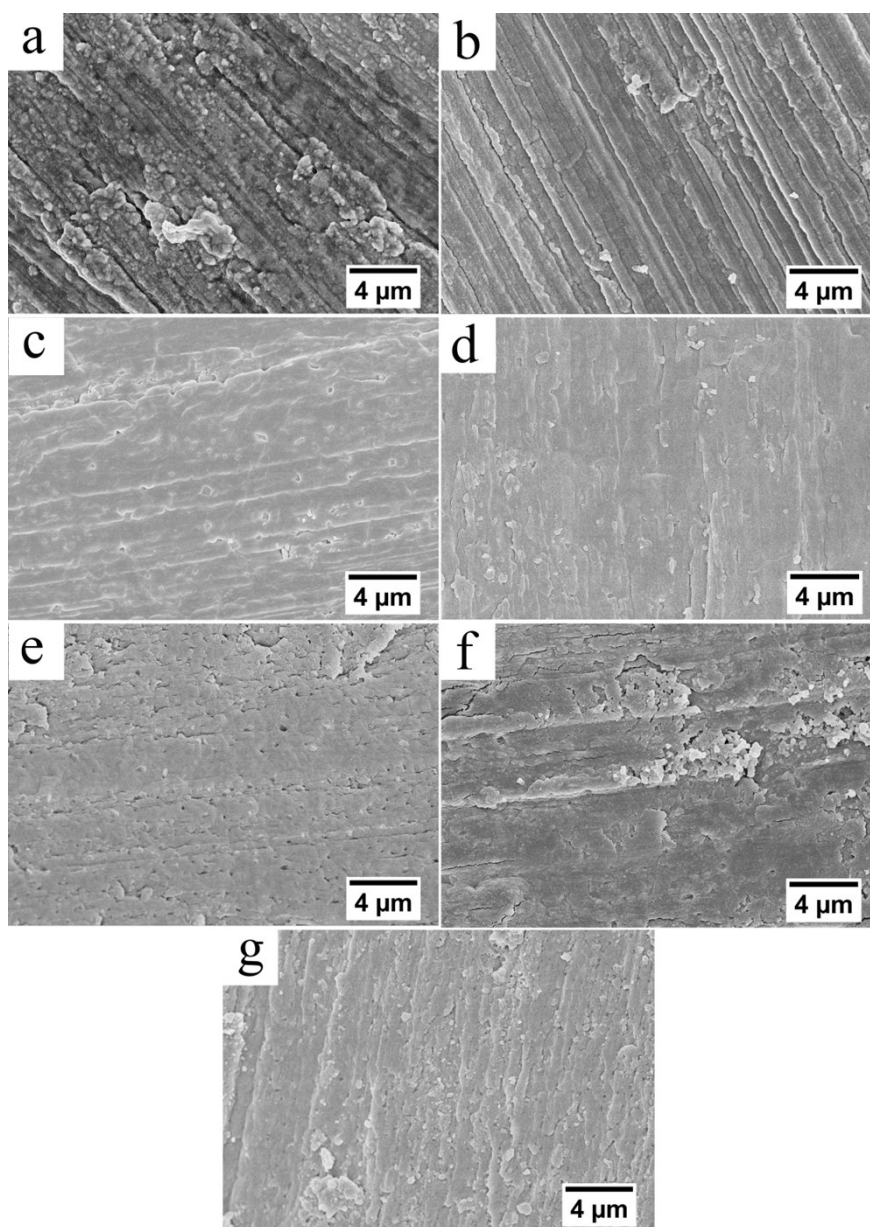


**Fig. S7** SEM images of the Li anodes after 20-cycle pre-activation at  $0.5 \text{ A g}^{-1}$  with different capacities of: a —  $25 \text{ mAh g}^{-1}$ ; b —  $50 \text{ mAh g}^{-1}$ ; c —  $100 \text{ mAh g}^{-1}$ ; d —  $400 \text{ mAh g}^{-1}$ ; e —  $500 \text{ mAh g}^{-1}$ ; f —  $800 \text{ mAh g}^{-1}$ ; g —  $1000 \text{ mAh g}^{-1}$ .

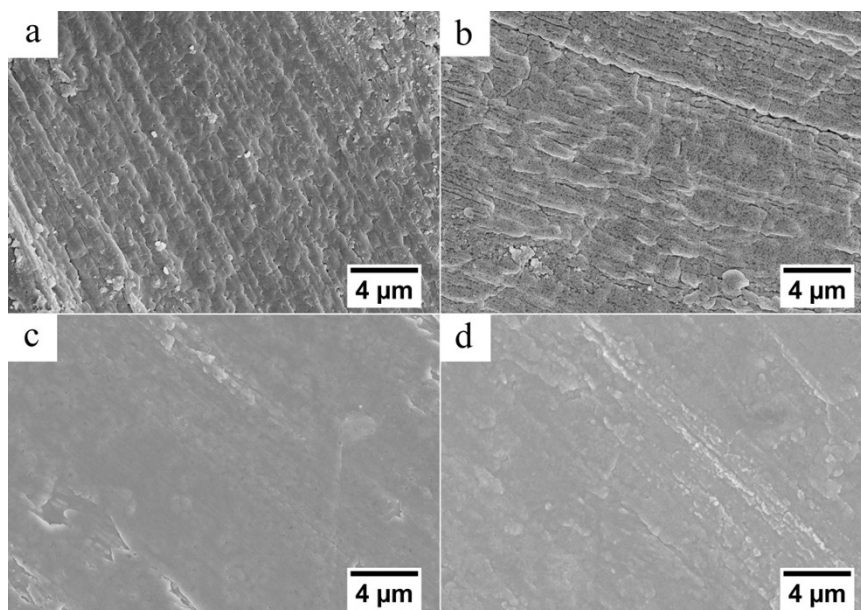


**Fig. S8** SEM images of the Li anodes after pre-activation at  $0.5 \text{ A g}^{-1}$  with a capacity of  $200 \text{ mAh g}^{-1}$  for different cycles of: a – 5; b – 10; c – 30; d – 40.

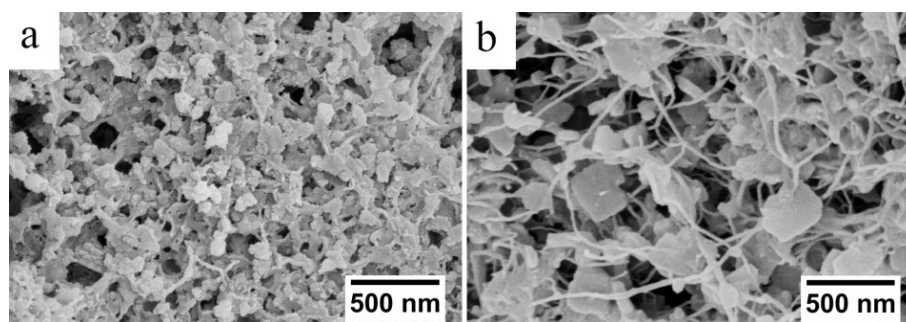


**Fig. S9** SEM images of the MWNTs cathodes in the cells without pre-activation (a) and with pre-activation (b) at the 1<sup>st</sup> cycle of battery testing.

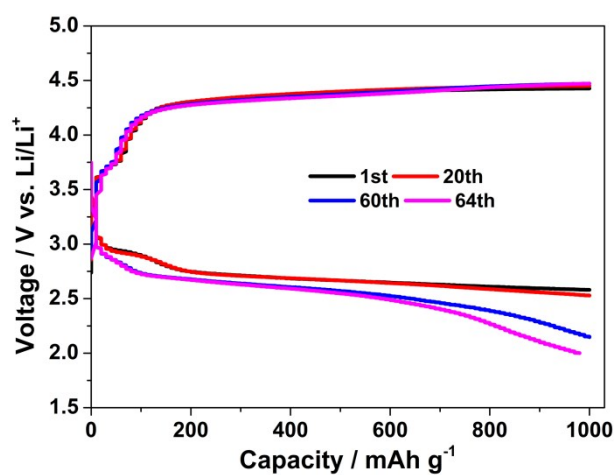


**Fig.S10** Charge/discharge profiles of the re-assembled battery with the used MWNTs after 290-cycle battery testing and a new Li anode.

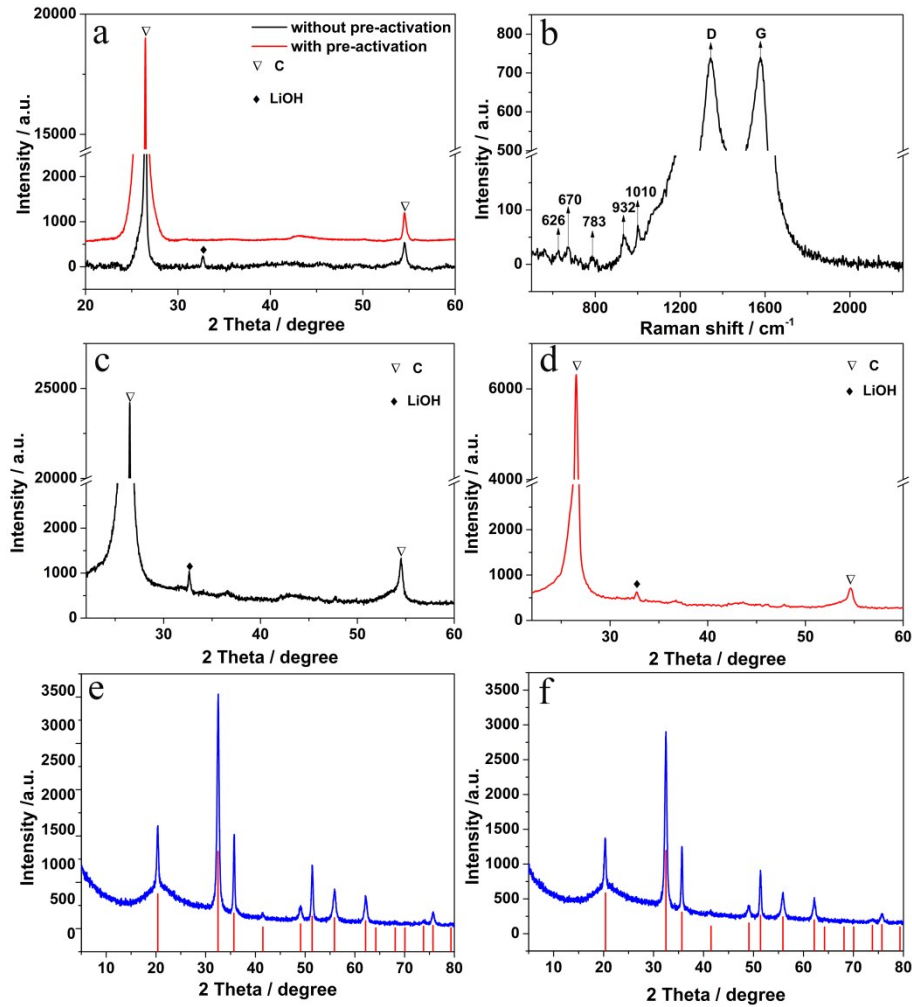


**Fig.S11** XRD and Raman analyses: a — XRD curves of the MWNTs cathodes for the cells cycled at  $1 \text{ A g}^{-1}$  and  $1000 \text{ mAh g}^{-1}$  or at  $0.5 \text{ A g}^{-1}$  and  $200 \text{ mAh g}^{-1}$  for 20 times; b — Raman analysis of the MWNTs cathode after pre-activation, where the peaks at  $626 \text{ cm}^{-1}$  and  $783 \text{ cm}^{-1}$  attributed to LiOH and  $\text{Li}_2\text{O}_2$ , and the peaks at  $1343 \text{ cm}^{-1}$  and  $1578 \text{ cm}^{-1}$  are associated to the D and G modes of MWNTs, and the peaks at  $670 \text{ cm}^{-1}$ ,  $932 \text{ cm}^{-1}$  and  $1010 \text{ cm}^{-1}$  are assigned to DMSO,  $\text{LiClO}_4$  and DME, respectively; c — XRD profile of the MWNTs cathode without pre-activation at the 55<sup>th</sup> cycle of battery testing; d — XRD profile of the MWNTs cathode with pre-activation at the 55<sup>th</sup> cycle of battery testing; e — XRD profile of the powder collected from the anode without pre-activation at the 55<sup>th</sup> cycle of battery testing; f — XRD profile of the powder collected from the anode with pre-activation at the 55<sup>th</sup> cycle of battery testing.

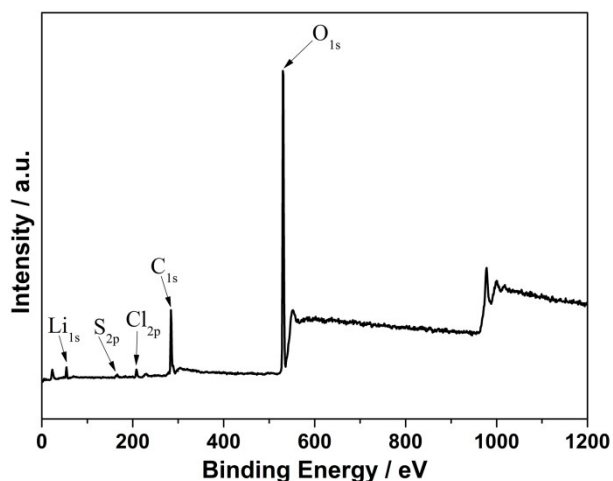


**Fig. S12** XPS total survey of the Li anode after 20-cycle pre-activation at  $0.5 \text{ A g}^{-1}$  with a capacity of  $200 \text{ mAh g}^{-1}$  for 20 cycles.

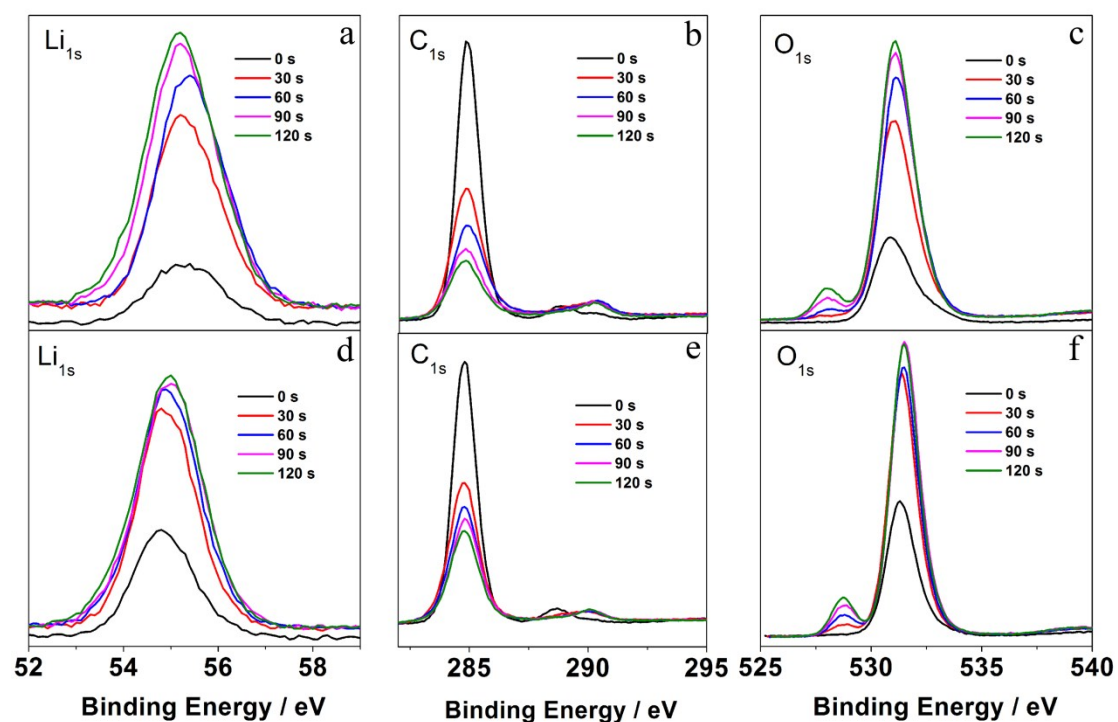


**Fig. S13** XPS in-depth profiling of  $\text{Li}_{1s}$ ,  $\text{C}_{1s}$  and  $\text{O}_{1s}$  signals in the cell cycled at  $1 \text{ A g}^{-1}$  with a capacity of  $1000 \text{ mAh g}^{-1}$  for 20 cycles (a, b, c), and in the cell cycled  $0.5 \text{ A g}^{-1}$  with a capacity  $200 \text{ mAh g}^{-1}$  for 20 cycles (d, e, f, with pre-activation).

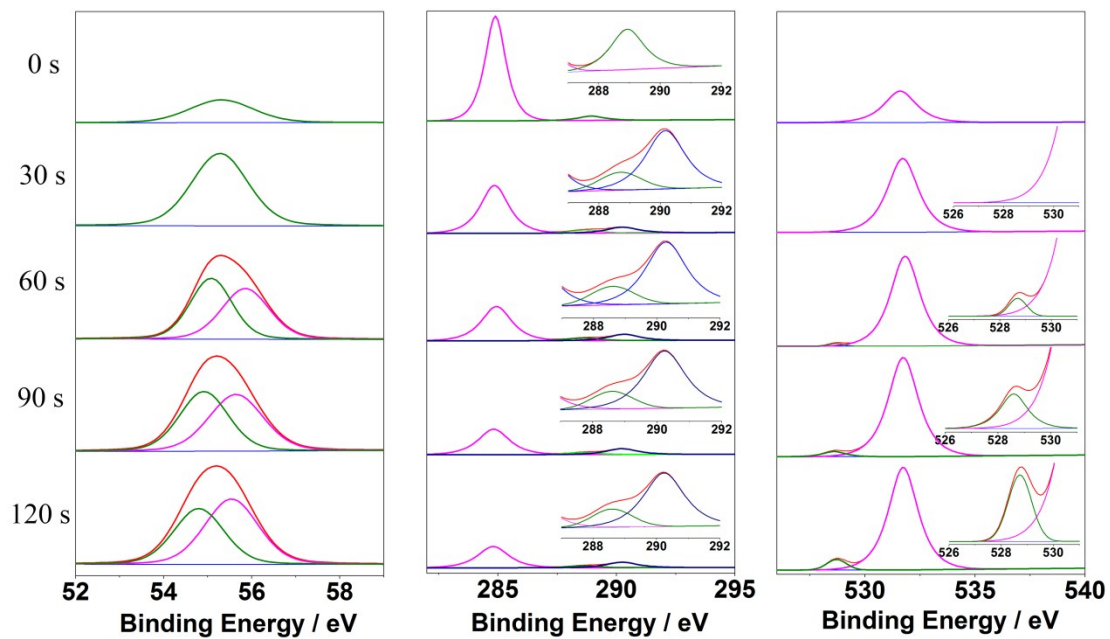


**Fig. S14** Sputtering time dependence of XPS spectra of the Li anode for the cell cycled at 1 A g<sup>-1</sup> with a capacity of 1000 mAh g<sup>-1</sup> for 20 times: left– Li<sub>1s</sub>; middle – C<sub>1s</sub>; right – O<sub>1s</sub>.

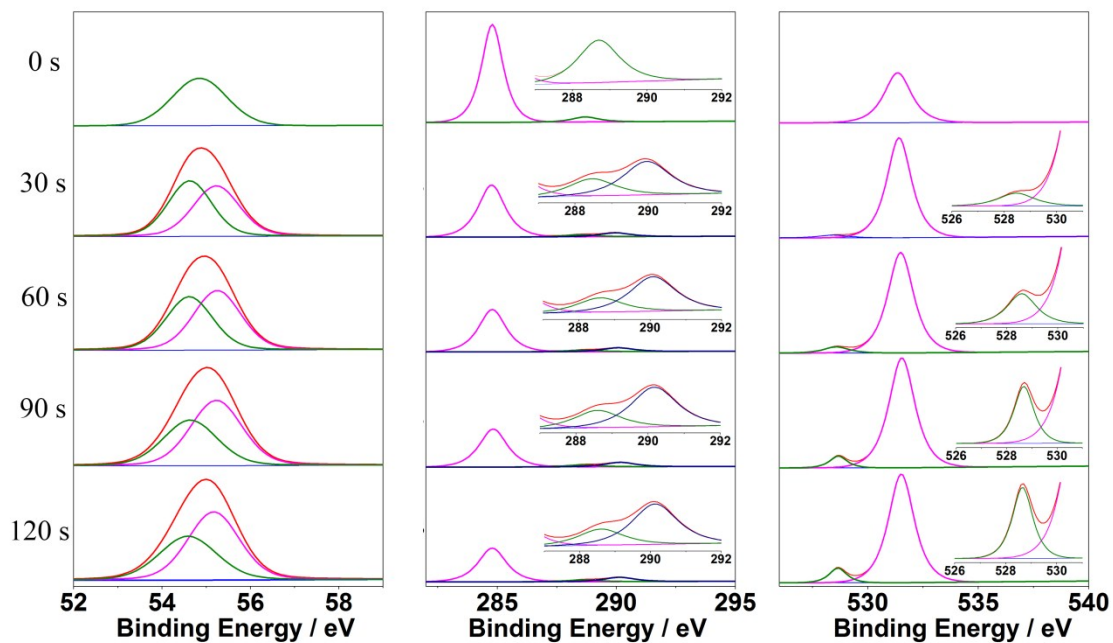


**Fig. S15** Sputtering time dependence of XPS spectra of the Li anode for the cell cycled at 0.5 A g<sup>-1</sup> with a capacity of 200 mAh g<sup>-1</sup> for 20 times (pre-activation) : left– Li<sub>1s</sub>; middle – C<sub>1s</sub>; right – O<sub>1s</sub>.

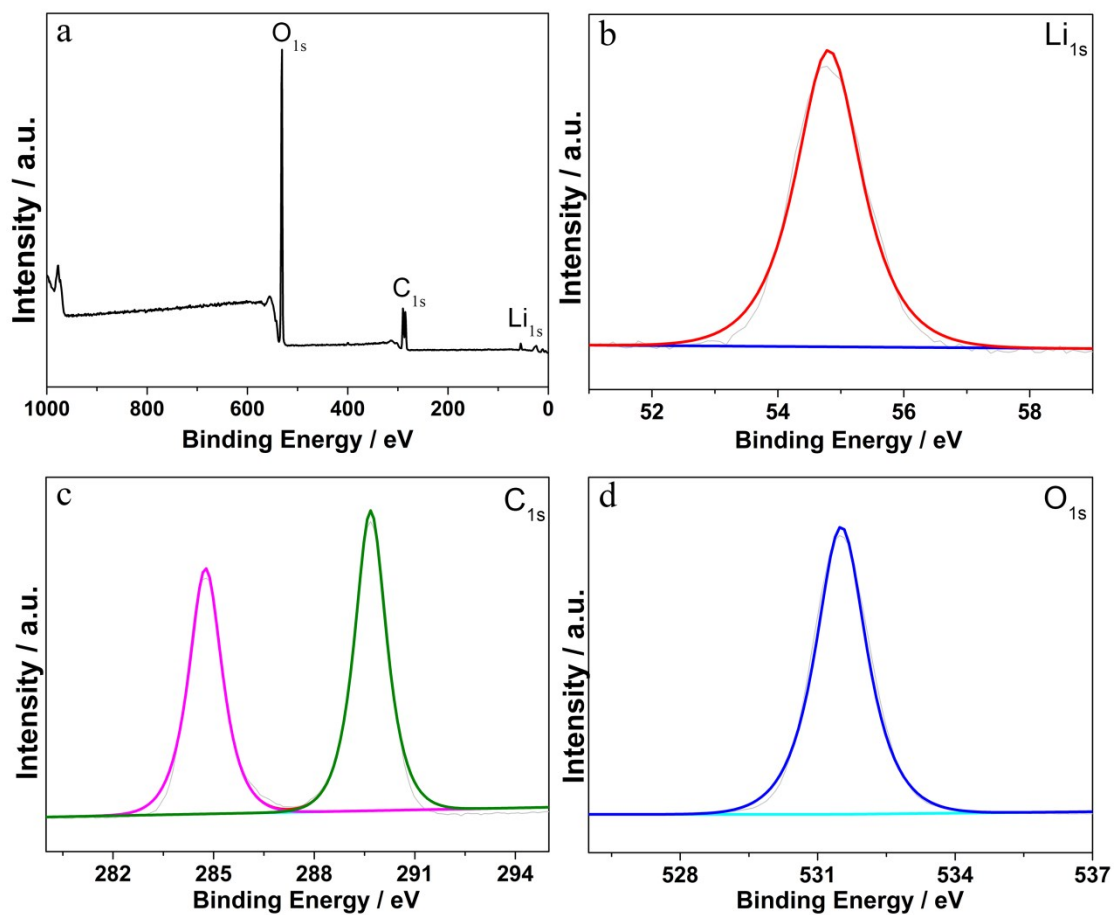


**Fig.S16** XPS total survey (a) and the fitting of the resolved Li<sub>1s</sub> (b), C<sub>1s</sub> (c) and O<sub>1s</sub> (d) signals of the standard Li<sub>2</sub>CO<sub>3</sub>.